Real time optical method for localization of inclusions embedded in turbid media

Anabela da Silva, Nadia Djaker, Nicolas Ducros, Jean-Marc Dinten, Philppe Rizo

▶ **To cite this version:**

HAL Id: hal-00875195
https://hal.archives-ouvertes.fr/hal-00875195

Submitted on 21 Oct 2013

Real time optical method for localization of inclusions embedded in turbid media

Anabela Da Silva[*(1,2)], **Nadia Djaker**[(1,2)], **Nicolas Ducros**[(1,3)], **Jean-Marc Dinten**[(1)], **and Philippe Rizo**[(1)]

[1]*CEA, LETI, micro-Technologies for Biology and Healthcare Division, 17 rue des Martyrs, F38054 Grenoble Cedex 9, France*
[2]*Institut Fresnel, CNRS, Aix-Marseille Université, Ecole Centrale Marseille, Campus de St Jérôme, 13013 Marseille, France*
[3]*CREATIS-LRMN, INSERM U 630; CNRS UMR 5220; Université de Lyon; INSA de Lyon, bât. Blaise Pascal, F-69621 Villeurbanne Cedex, France.*
[*] *anabela.dasilva@fresnel.fr*

Abstract: A simple and fast time-domain method for localizing inclusions, fluorescent optical probes or absorbers, is presented. The method offers new possibilities for situations where complete tomographic measurements are not permitted by the examined object, for example in endoscopic examination of the human prostate or the oesophagus. The feasibility has been envisioned with a phantom study conducted on a point-like fluorochrome embedded in a diffusing medium mimicking the optical properties of biological tissues.

OCIS codes: 170.5280 (Photon migration); 170.3660 (Light propagation in tissues); 170.7050 (Turbid media); 170.6920 (Time-resolved imaging); 300.2530 (Fluorescence, laser-induced); 170.3880 (Medical and biological imaging).

References

1. A. Yodh and B. Chance, Phys. Today **48**, 34 (1995).
2. T. Austin, A.P. Gibson, G. Branco, R.M. Yusof, S.R. Arridge, J.H. Meek, J.S. Wyatt, D.T. Delpy, J.C. Hebden, Neuroimage **30**, 88 (2006).
3. L.C. Enfield, A.P. Gibson, N.L. Everdell, D.T. Delpy, M. Schweiger, S.R. Arridge, C. Richardson, M. Keshtgar, M. Douek, J.C. Hebden, Applied Optics **46**, 3628 (2007).
4. D. Piao, H. Xie, W.L .Zhang, J.S. Krasinski, G.L. Zhang, H. Dehghani, B.W. Pogue, Optics Letters **31**, 2876 (2006).
5. Y.-F. Chang and C.-Y. Wang, Journal of Nondestructive Evaluation, **16**, 193 (1997).
6. R. Aronson, and N. Corngold, Journal of the Optical Society of America a-Optics Image Science and Vision **16**, 1066 (1999)
7. A. Laidevant, A. Da Silva, M. Berger, J. Boutet, J.-M. Dinten, and A. C. Boccara, Applied Optics **46**, 2131 (2007)
8. A. Laidevant, A. Da Silva, M. Berger, and J.-M. Dinten, Applied Optics **45**, 4756 (2006)
9. A. Pifferi, A. Torricelli, L. Spinelli, D. Contini, R. Cubeddu, F. Martelli, G. Zaccanti, A. Tosi, A. Dalla Mora, F. Zappa, and S. Cova, Phys. Rev. Lett. **100**, 138101 (2008).
10. J. Boutet, L. Guyon, M. Debourdeau, J.-M. Dinten, D. Vray, P. Rizo, Proc. SPIE Vol. 7171, Multimodal Biomedical Imaging IV, F. S. Azar, X. Intes, Editors (2009)

1. Introduction

The interest in optical techniques for biological tissues screening has grown in the last decade because they represent a non invasive and non ionizing method for diagnosis or imaging [1]. Diffuse Optical Tomography (DOT) systems are declined into three categories, according to the illumination light: i) continuous wave; ii) intensity modulated; iii) pulsed illumination. Time resolved techniques are those who carry the richest information on the optical properties of the crossed tissue, and seem to be those that are more suitable for deep tissue screening (several centimeters for brain or breast examination) [2,3]. However, they are also those for

which the reconstruction techniques are the most sophisticated and become sometimes intractable for real time resolution of the inverse problem. Classical photon migration measurements consist in illuminating a diffusing medium (biological tissues) with a point-like source and collecting the reemitted optical signal at a given distance from the injection point. The distribution of the diffuse photons depends on the optical properties (absorption and diffusion) of the screened medium. At each point, the measurement is a time depending function called Temporal Point Spread Function (TPSF). The stake of the problem is to extract simple signatures from the TPSF, whose one knows the theoretical expression (thanks to a forward model connecting the unknowns and these temporal signatures). Then, the resolution of the inverse problem leads to the determination of the unknowns, that can be the three-dimensional (3D) distribution of the optical parameters (absorption and diffusion coefficients) in DOT or/and the properties of an optical probe (concentration, lifetime), such as in Fluorescence DOT (FDOT). Nowadays, the trend is to increase the number of measurements with large numbers of sources and detectors positions for a better resolution, which leads to very complex systems, with long acquisition times, and to memory consuming inverse problems leading to computation times not compatible with real time imaging.

The problem we address in this paper is that, sometimes, the object or the body to be examined simply prohibits the use of many sources and detectors, for example in endoscopy for the examination of the prostate or the oesophagus [4].

The principle is inspired by the method of localization and imaging of cracks in concrete structures by ultrasounds [5]. The method exposed here is rewritten within the framework of FDOT, for a 3D localization of a fluorescent zone embedded in a diffusive volume, but it can be transcripted for localizing an absorbing inclusion after a linearization step of the problem by using a perturbation approach. The equations for the fluorescence process are usually derived by considering a two step approach according to the Jablonski diagram: i) a photon is absorbed at the excitation wavelength λ_x; ii) the photon is reemitted, after a delay called the fluorescence lifetime τ, at a higher wavelength λ_m. With the same phenomenological description, absorption can be seen as a simplified fluorescence process: once absorbed, a photon is immediately reemitted ($\tau = 0$), at the same wavelength λ_x.

Basically the method allows a localization of the fluorescent inclusions without reconstruction, with a limited number of sources and detectors points.

2. Derivation of the method

We consider the normalized time moments, m_k, of the TPSF, noted ϕ_m, and defined as:

$$m_k = \int_{-\infty}^{+\infty} t^k \phi_m(r,t)dt \bigg/ \int_{-\infty}^{+\infty} \phi_m(r,t)dt = <t^k>$$

$$= (i)^k \frac{\partial^k \tilde{\Phi}(\omega)}{\partial \omega^k}\bigg|\omega = 0 \times \frac{1}{\tilde{\Phi}(\omega)|\omega = 0}$$

(1)

$\tilde{\Phi}(\omega)$ is the Fourier transform of ϕ_m. In all what follows, the equations will be written by considering an infinite diffusing medium, but similar expressions can be found for slightly more complicated geometries such as semi-infinite media or slabs. Generally speaking, if the expression of $\tilde{\Phi}(\omega)$ is known, analytically or numerically, one can use the second relation in (1) for easily calculating m_k. One can demonstrate that, if the diffusing medium is infinite, the first order moment m_1 defining the mean time of flight $<t>$ of the fluorescence photons can be written as:

$$m_1 = <t>_\infty = <t>_x + <t>_m + \tau = \frac{|\mathbf{r_s} - \mathbf{r}|}{v_x} + \frac{|\mathbf{r} - \mathbf{r_d}|}{v_m} + \tau \qquad (2)$$

$$v_{x,m} = 2c_n\sqrt{\mu_{ax,m}D_{x,m}}$$

$<t>_x$ (respectively $<t>_m$) represents the mean time-of-flight of the photons traveling at the excitation (resp. emission) wavelength from the source point located at $\mathbf{r_s}$ to the fluorescence inclusion at $\mathbf{r}$ (resp. from the fluorescence inclusion at $\mathbf{r}$ to the detector at $\mathbf{r_d}$); τ is the lifetime of the fluorochromes; c_n is the speed of light in the medium, $\mu_{ax,m}$ [m^{-1}] is the absorption coefficient and $D_{x,m}$ [m] is the diffusion coefficient at the excitation/emission wavelength, appearing in the diffusion equation as derived within the Diffusion Approximation to the Radiative Transport Equation [6]. $v_{x,m}$ thus represents the apparent speed of light within the diffusing medium at the excitation/emission wavelength.

As an unusual case, by considering the same optical properties at both the excitation and emission wavelengths, which is an assumption sometimes achieved when the excitation and emission wavelengths are close (few tens of nm), one obtains:

$$|\mathbf{r_s} - \mathbf{r}| + |\mathbf{r} - \mathbf{r_d}| = v(<t>_\infty - \tau) = d \qquad (3)$$

The above equation describes the 3D surface of an ellipsoid with focal points located at $\mathbf{r_s}$ and $\mathbf{r_d}$, and its solution is the set of points $\mathbf{r}$ such that distance source-fluorochrome $|\mathbf{r_s} - \mathbf{r}|$ plus distance fluorochrome-detector $|\mathbf{r} - \mathbf{r_d}|$ is equal to a constant, noted in the present case d. This constant corresponds to the apparent speed of light in the diffusing medium v multiplied by the mean time-of-flight corrected by the delay introduced by the lifetime τ. In other words, the location of a fluorochrome providing the measurement value $m_1 = <t>_\infty$ belongs to this 3D surface. By increasing the number of measurements (at least three in 3D), and by searching the intersection between the set of the resulting 3D surfaces, one obtains the set of the possible positions of the fluorochrome.

Higher order moments can be considered. For instance, with the second order moment, one can build the time variance expressed as $<(t - <t>)^2> = m_2 - m_1^2$, and one can also find that the resulting equation is also the 3D surface of an ellipsoid. Note that if the problem is reduced to the location of an absorbing object, the 3D surface defining the set of the solutions is obtained by setting $\tau = 0$ in equation (3).

In the general case, the optical properties at the excitation and emission wavelengths are different. Equation (2) still defines a 3D surface, and the idea is still to increase the number of measurements in order to find the intersection between the different 3D surfaces generated by each measurement. Note that the location of a fluorochrome depends on the lifetime, which is a parameter known to be sensitive to the biological environment. To get rid of this, one can consider differential measurements as detailed in Ref. [7]. In this case, at least four measurements have to be considered, one of them dedicated to the reference measurement.

3. Experimental implementation

The experimental setup used (Fig. 1) is described in detail elsewhere [7]. A picosecond laser diode operating at wavelength 635 nm with a repetition rate of 50 MHz (BHL-600, Becker&Hickl, Germany) is used for the study. The laser beam is injected in an excitation optical fiber to illuminate the sample; the average power is about 100 µW. The scattered reflected optical signal from the sample is collected by the detection optical fiber coupled to a fast photomultiplier tube (R3809U-50, Hamamatsu Photonics, Japan). A Time-Correlated Single Photon Counting (TCSPC) system (SPC-630, Becker&Hickl, Germany) is used to obtain time-dispersion curves. The TCSPC computer card is synchronized by a reference

signal generated inside the laser diode box. The sample consists of a plastic cylindrical tank filled with a water solution of intralipid (Fresenius, France) as the scattering medium. By exploiting the time-dependent diffusion equation for an infinite homogeneous medium:

$$\frac{1}{c_n}\frac{\partial}{\partial t}\phi(\mathbf{r},t) - \nabla.(D(\mathbf{r})\nabla\phi(\mathbf{r},t)) + \mu_a(\mathbf{r})\phi(\mathbf{r},t) = S(\mathbf{r},t), \tag{4}$$

with $\phi(\mathbf{r},t)$ proportional to the measured TPSF, and $S(\mathbf{r},t)$ the spatio-temporal intensity of the pulse laser signal, the optical properties of the sample turn out to be $D=3.83\text{x}10^{-2}$ cm and $\mu_a=0.01$ cm^{-1} at the excitation wavelength. The optical properties are assumed to be the same at the emission wavelength. The fluorescent inclusion consists on two microliters of Cy5 fluorochrome (concentration 10 µM, Molecular Probes, Invitrogen, USA) placed at the tip of a thin glass capillary tube (3 cm long, 1 mm thick). The fluorescence lifetime is τ =1.1 ns. The tube was inserted into the tank through a hole drilled in the bottom (see inset Fig. 1).
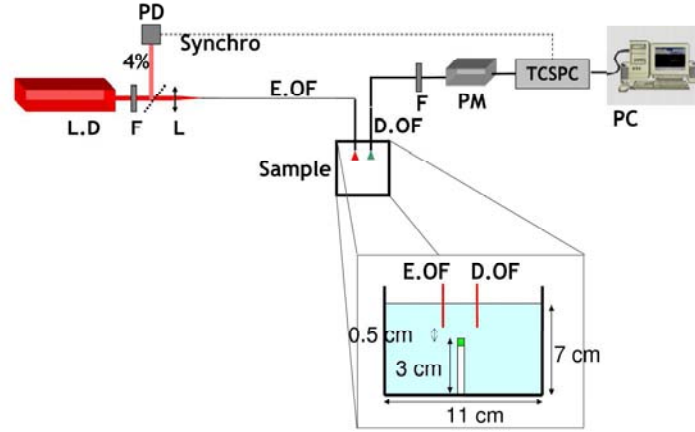

Fig. 1: Experimental time resolved setup. L.D.: Laser Diode; F: Filters; L: lens; PD: photodiode; E.OF: excitation optical fiber; D.OF: detection optical fiber; PM: photomultiplier; TCSPC: time correlated single photon counting system.

Experimental data were recorded at different positions between the fibers and the fluorescent inclusion in space (XYZ) (see Fig. 2). For each case, the fibers were embedded at 3.5 cm into the medium. This distance was found to be sufficient to achieve the infinite medium geometry required [8]. The distance between the fibers plane and the fluorescent inclusion is set at 0.5 cm. The light is driven from a laser by an optical fiber, the beam is infinitely narrow. It is commonly admitted that the system is equivalent to an isotropic source placed at a distance of one transport mean free path from the actual source, that is, in the present case 0.11 cm from the tip of the fiber. Five different configurations of source (S) and detector (D), reported on Fig. 2a, have been considered for this experiment.
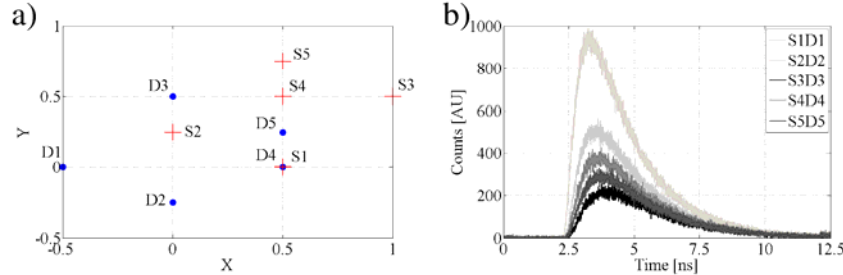

Fig. 2 : (a) Relative positions of the five different couples of source (cross markers) and detector (plain dot markers); (b) TPSFs of the five selected measurements.

The corresponding measured TPSF are presented on Fig. 2b, right, resulting in the following calculated values of the distance $d =$(2.27; 2.01; 2.73; 2.39; 2.53) cm. Note that the measured curves have been preprocessed as recommended in Ref. [7].

For solving the inverse problem, the medium is meshed into voxels. In the present case, the mesh chosen is defined as follows: X direction, 50 nodes from -0.5 to 2 cm; Y direction, 30 nodes from -0.5 to 1 cm; Z direction, 50 nodes from -6 to -3.5 cm (corresponding to cubic voxels of size 0.05 cm). Fig. 3 presents an example of 3D surface defined by the set of points solution of equation (3) for the measurement S1D1. In the present case, as the medium is supposed to be infinite and the optical properties are the same at the excitation and emission wavelengths, the 3D surface describes an ellipsoid.

Among the available measurements, we first considered three of them and find the intersection of the sets of solutions of the three corresponding equations. Fig. 4 illustrates the three corresponding ellipsoids, and their intersections corresponding to the experimentally determined position of the point-like fluorochrome. The computation time for the chosen mesh is less than 3 s (computation of distance d for the 3 measurements 2.6 s, computation of the three ellipsoids 0.12 s and determination of the intersection 0.04 s, with Matlab® software, and processor Intel Core2, 2.13GHz, 1Gb RAM).

The fluorochrome was found to be located at $(-0.066<x<0.087, 0.095<y<0.195, -3.935<z<-3.785)$ cm while the actual position is (0,0,-4) cm. We then considered the whole set of five measurements. The results are reported on Fig. 5. The fluorochrome was found to be located at $(0.035<x<0.085, 0.095<y<0.145, -3.935<z<-3.885)$ cm which is a slightly more refined solution.
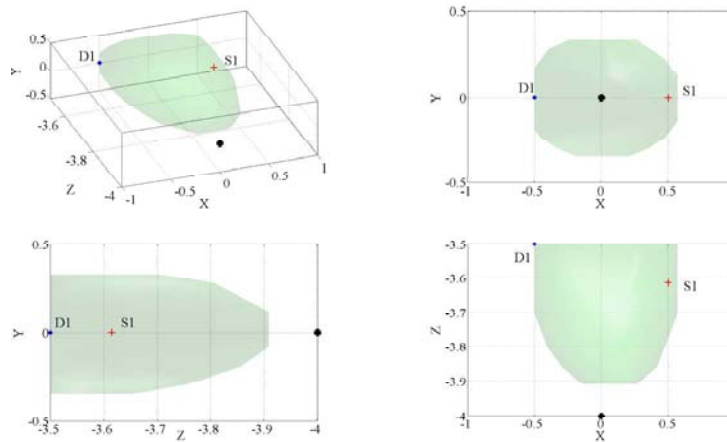

Fig. 3 : Different point of views of the 3D surface defined by the set points solution of equation (3) for the measurement S1D1.

The method is very versatile and shows up the possibility to adopt multiresolution schemes, according to the expected resolution. One can note that if source and detector are very close, in an infinite medium, according to Eq. (3), the 3D surface described becomes a sphere. This configuration has been recently mentioned to be a very advantageous situation for photon migration measurements [9], when deep tissue screening is envisioned. This can be performed, provided a time gating is applied on the TPSF measurement for rejecting early-arriving photons that do not meet the requirements for using the diffusion approximation.
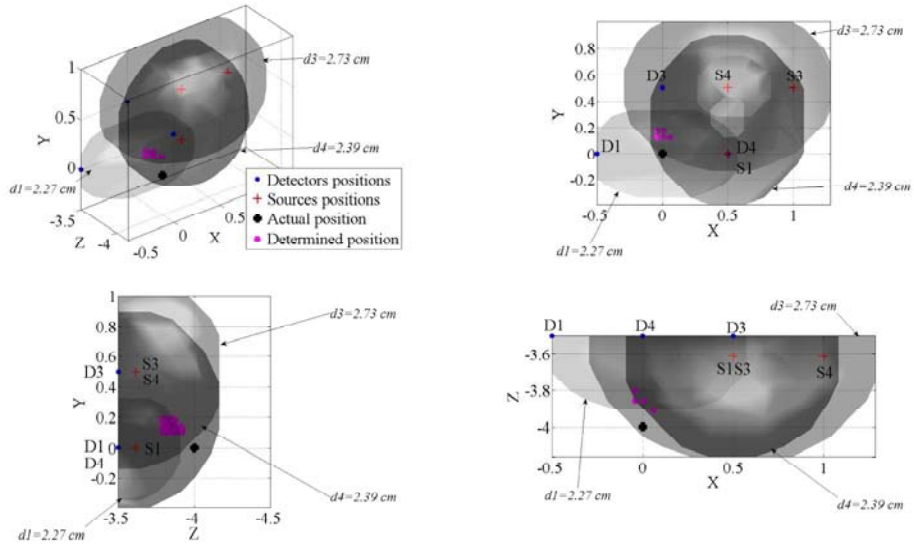
Fig. 4: Different points of view of the 3D surfaces for the measurement S1D1 (d1=2.27 cm), S3D3 (d3=2.73 cm) and S4D4 (d4=2.39 cm) merged with the actual position (plain dot marker) and the position of the fluorochrome defined by the intersection of the three 3D surfaces (star markers).
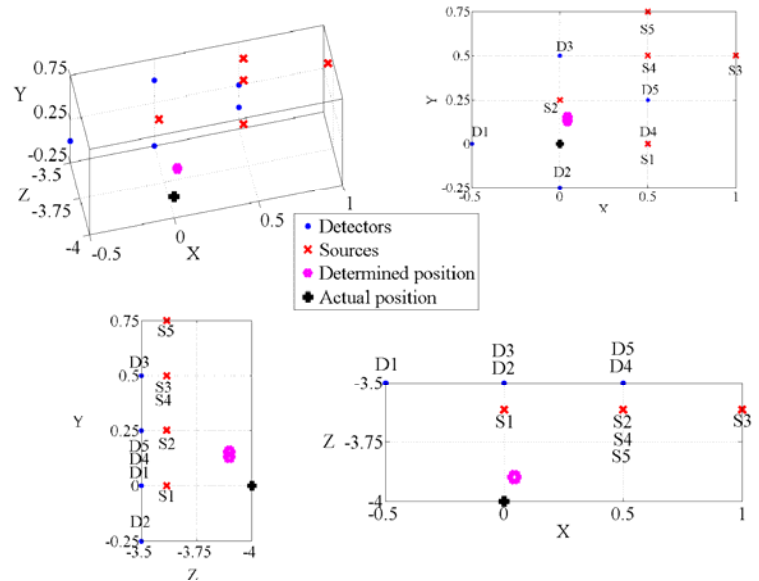

Fig. 5: Different points of view of the position of the fluorochrome (star markers) defined by the intersection of the whole set of measured 3D surfaces (not plotted); the actual position is represented as a plain cross marker.

4. Conclusion

We have exposed a fast and accurate method for real time localization of compact absorbing or fluorescing zones embedded within turbid media. For simplicity, the demonstration, theoretical and experimental, has been conducted assuming a homogeneous diffusing and absorbing infinite medium as the host medium. For a semi-infinite medium, which is a more practical situation for *in vivo* experiments, an analytical expression can still

be easily derived for the mean time-of-flight as a function of the distances $|\mathbf{r}_s - \mathbf{r}|$ and $|\mathbf{r} - \mathbf{r}_d|$. Nevertheless, the whole derivation relies on the knowledge of the expression of the Fourier transform $\tilde{\Phi}(\omega)$ in expression (1), that can be computed numerically for a non homogeneous medium, with arbitrary shape, allowing a generalization of the method. The 3D resulting surfaces would be more complicated than simple ellipsoids.

Overall, our findings demonstrate the experimental feasibility of the approach for diagnosis, opening new investigation directions in the field of photon migration based approaches of diagnostics and imaging. For instance it can be easily coupled with an ultrasound transrectal probe and used for guiding the biopsies in prostate cancer detection or therapy [10].

The method is however limited to the localization of a single object and does not provide quantitative measurements. Its robustness has to be studied especially when the contrast between the background and the target is weak. This method is otherwise very easy to introduce as an initialization step in a more sophisticated reconstruction algorithm.